Molecular Neurobiology (2018) 55:9156–9168
https://doi.org/10.1007/s12035-018-1063-3

Improved Reperfusion and Vasculoprotection by the Poly(ADP-Ribose) Polymerase Inhibitor PJ34 After Stroke and Thrombolysis in Mice

Mohamad El Amki[1] · Dominique Lerouet[1] · Marie Garraud[1] · Fei Teng[1] · Virginie Beray-Berthat[1] · Bérard Coqueran[1] · Benoît Barsacq[1] · Charlotte Abbou[1] · Bruno Palmier[1] · Catherine Marchand-Leroux[1] · Isabelle Margaill[1]

Received: 4 February 2018 / Accepted: 3 April 2018 / Published online: 12 April 2018

Abstract

Benefits from thrombolysis with recombinant tissue plasminogen activator (rt-PA) after ischemic stroke remain limited due to a narrow therapeutic window, low reperfusion rates, and increased risk of hemorrhagic transformations (HT). Experimental data showed that rt-PA enhances the post-ischemic activation of poly(ADP-ribose)polymerase (PARP) which in turn contributes to blood-brain barrier injury. The aim of the present study was to evaluate whether PJ34, a potent PARP inhibitor, improves poor reperfusion induced by delayed rt-PA administration, exerts vasculoprotective effects, and finally increases the therapeutic window of rt-PA. Stroke was induced by thrombin injection (0.75 UI in 1 μl) in the left middle cerebral artery (MCA) of male Swiss mice. Administration of rt-PA (0.9 mg kg^{-1}) or saline was delayed for 4 h after ischemia onset. Saline or PJ34 (3 mg kg^{-1}) was given intraperitoneally twice, just after thrombin injection and 3 h later, or once, 3 h after ischemia onset. Reperfusion was evaluated by laser Doppler, vascular inflammation by immunohistochemistry of vascular cell adhesion molecule-1 (VCAM-1) expression, and vasospasm by morphometric measurement of the MCA. Edema, cortical lesion, and sensorimotor deficit were evaluated. Treatment with PJ34 improved rt-PA-induced reperfusion and promoted vascular protection including reduction in vascular inflammation (decrease in VCAM-1 expression), HT, and MCA vasospasm. Additionally, the combined treatment significantly reduced brain edema, cortical lesion, and sensorimotor deficit. In conclusion, the combination of the PARP inhibitor PJ34 with rt-PA after cerebral ischemia may be of particular interest in order to improve thrombolysis with an extended therapeutic window.

Keywords Stroke · Recombinant tissue plasminogen activator · Reperfusion · Vasculoprotection

Abbreviations

BBB	Blood-brain barrier
CBF	Cerebral blood flow
DAB	3,3′-Diaminobenzidine tetrahydrochloride
MCA	Middle cerebral artery
PARP	Poly(ADP-ribose)polymerase
PJ34	*N*-(6-Oxo-5,6-dihydrophenanthridin-2-yl)-(*N*,*N*-dimethylamino)acetamide hydrochloride
ROI	Region of interest
rt-PA	Recombinant tissue plasminogen activator
VCAM-1	Vascular cell adhesion molecule-1

✉ Isabelle Margaill
isabelle.margaill@parisdescartes.fr

[1] EA4475 - "Pharmacologie de la Circulation Cérébrale", Faculté de Pharmacie de Paris, Université Paris Descartes, Université Sorbonne Paris Cité, 4 avenue de l'Observatoire, 75006 Paris, France

Introduction

Thrombolysis with recombinant tissue plasminogen activator (rt-PA) remains the only approved pharmacological strategy for acute ischemic stroke. However, less than 2% patients can benefit from this treatment due to several reasons [1]. First, rt-PA has limited thrombolytic efficiency and low recanalization rates especially in large artery occlusions [2, 3]. Additionally, rt-PA has a narrow therapeutic window (4.5 h) after stroke symptom onset [4]. Beyond this limit, rt-PA is devoid of beneficial effects. Furthermore, rt-PA increases the risk of hemorrhagic transformations [5].

Poly(ADP-ribose)polymerases (PARPs) are a large family of nuclear enzymes within which PARP-1 accounts for about 90% of PARP activity [6]. PARP-1 physiologically exerts beneficial effects as this enzyme participates in DNA repair, cell cycle control, and genomic stability [7]. However PARP overactivation is deleterious in experimental models of cerebral ischemia in rodents [8–10] and primates [11]. Excessive

activation of PARP-1 indeed leads to cellular NAD and ATP depletion, neuroinflammation, apoptosis inducing factor (AIF) translocation from mitochondria to nucleus, and ultimately neuronal cell death through necrosis, autophagy, or parthanatos (a caspase-independent programmed cell death induced by AIF) [12, 13].

Interestingly, rt-PA was reported to increase PARP activation in a model of permanent focal cerebral ischemia induced by mechanical occlusion of the middle cerebral artery (MCA) in mice [14]. In the same model of permanent MCA occlusion, we showed, using the potent PARP inhibitor PJ34 given at stroke onset, that PARP contributes to rt-PA-induced blood-brain barrier (BBB) breakdown and hemorrhagic transformations [8, 9]. Additionally, several studies reported that PARP inhibition suppresses the post-stroke neuroinflammation and thereby induces neuroprotection [15–17]. However, even though there is a wealth of research about the role of PARP inhibitors on the brain inflammation, BBB disruption, and hemorrhagic transformations, their effect on the post-ischemic reperfusion and the vascular inflammation induced by rt-PA has not been studied in stroke.

The present study examined the effect of PJ34 and rt-PA in a thromboembolic model of cerebral ischemia in which reperfusion can occur. This model is particularly relevant to examine strategies to be associated with rt-PA, as we previously reported that delaying administration of rt-PA (4 h after ischemia onset) in this model leads, as in clinic, to decreased reperfusion and loss of neuroprotection [18]. We took advantage of this model to study the impact of associating both compounds on reperfusion, vascular inflammation, and cerebral vasospasm (that has been extensively studied in subarachnoid hemorrhage as a contributor of poor outcome and death [19] but poorly investigated after ischemic stroke). Finally, in this model, we evaluated whether restoration of cerebral blood flow (CBF) and reduction of vascular injury after ischemia extend the therapeutic window of rt-PA by evaluating the infarct volume and neurological deficit.

Methods

Animals

All experiments were performed on male Swiss albino mice (25–32 g, Janvier, Le Genest-St-Isle, France) in compliance with the European Community Council Directive of September 22, 2010 (2010/63/UE), and the French regulations regarding the protection of animals used for experimental and other scientific purposes (D2013-118), with the ethical approval of the Paris Descartes University Animal Ethics Committee (registered number P2.CM.152.10). Mice were housed under standard conditions with a 12-h light/dark cycle and allowed access to food and water ad libitum. Animals were randomly assigned to experimental groups and treated in a blinded manner.

Focal Cerebral Ischemia

Male Swiss mice were intraperitoneally anesthetized with ketamine (50 mg kg^{-1}) and xylazine hydrochloride (6 mg kg^{-1}). Ischemia was induced by occlusion of the left MCA using a thromboembolic model [20]. In this model, we have previously evaluated the effects of thrombolysis on reperfusion in male Swiss albino mice [18]. After craniotomy and dura excision, a glass pipette was introduced into the lumen of the MCA and 1 μl of purified human alpha-thrombin (0.75 UI; HCT-0020, Hematologic Technologies Inc., Essex Junction, USA) was injected to induce the formation of a clot in situ. The same surgical procedure was performed in sham-operated mice, except the introduction of the pipette into the MCA. The CBF was monitored in the MCA region by laser Doppler flowmetry (Moor instruments, Millwey, UK); a clot was defined stable when CBF rapidly falls to at least 50% of the baseline level after the beginning of thrombin injection [21] and remains below this value for 30 min. Mice with less than a 50% drop or with spontaneous reperfusion were excluded. Body temperature was monitored throughout surgery by a rectal probe and maintained at 37 ± 0.5 °C with a homeothermic blanket control unit (Harvard Apparatus, Edenbridge, Kent, UK). After surgery, mice were returned to their home cage and fed mashed lab chow. In order to prevent from dehydration, mice received a subcutaneous injection of 0.5 ml saline the day of surgery.

Treatment Schedules

Mice received rt-PA (Actilyse®, Boehringer-Ingelheim, Biberach an der Reiss, Germany) intravenously (tail vein; 0.9 mg kg^{-1}; 10% bolus, 90% perfusion during 30 min) or its vehicle (saline) 4 h after ischemia [18]. PJ34 (3 mg kg^{-1}; P4365, Sigma-Aldrich, Saint Quentin Fallavier, France) or its vehicle (saline) was administered intraperitoneally twice, just after thrombin injection (0 h) and 3 h later according to our previous work [8, 9, 22], or once, 3 h after ischemia induction.

Effect of PJ34 and rt-PA on Acute Reperfusion

Ischemic mice were randomly assigned to one of the following groups ($n = 5$/group): (1) saline (at 0, 3, and 4 h post-ischemia), (2) rt-PA (and saline at 0 and 3 h), (3) PJ34 at 0 and 3 h plus rt-PA, and (4) PJ34 at 3 h plus rt-PA (and saline at 0 h). Thirty minutes after thrombin injection, mice were returned to their home cages maintained at 30 °C. Three hours post-ischemia, mice were re-anesthetized just before the administration of PJ34 or saline, and CBF was thereafter continuously monitored for 3 h. Quality of cerebral reperfusion was

assessed by the area under the curve (AUC) from 4 to 6 h. AUC was calculated by measuring the area under the CBF curve between the injection of rt-PA (4 h) and the end of CBF monitoring (6 h).

Effect of PJ34 and rt-PA on Ischemic Outcomes at 24 H

Ischemic mice were randomly assigned to one of the following five groups ($n = 19$–20/group): (1) saline (at 0, 3, and 4 h post-ischemia), (2) rt-PA (and saline at 0 and 3 h), (3) PJ34 at 0 and 3 h (plus saline at 4 h), (4) PJ34 at 0 and 3 h plus rt-PA, and (5) PJ34 at 3 h plus rt-PA (and saline at 0 h). Sham-operated mice ($n = 19$) were treated with saline at 0, 3, and 4 h after surgery.

Behavioral Tests

Behavioral tests were blindly performed 24 h after ischemia. Spontaneous locomotor activity was evaluated using an actimeter (Imetronic, Bordeaux, France) as previously described [23]. Mice were individually placed in actimeter cages, where lighting was fixed at 5 lx. Ambulatory activity and rearing were measured with the aid of photocell beams located across the long axis (detection of horizontal activity) and on the sides (detection of vertical activity) of each compartment, respectively. Animals were not preconditioned in the cages and their spontaneous locomotor activity was measured during 60 min. Results were expressed as the number of photocell beam disruptions per 60 min (counts/60 min) for horizontal and vertical activities.

Neurological deficit was evaluated using a global neurological score modified from [18]. Contralateral sensorimotor functions were examined through 3 items: the abnormal postures after tail suspension, the forelimb and hindlimb grasping reflexes performed onto a metallic wire, and the forelimb and hindlimb hanging reflexes. The scores for each item were summed and used as a global neurological score in which maximum was 8. Lower score reflects higher deficit.

Mice were then intraperitoneally anesthetized with sodium pentobarbitone (60 mg kg^{-1}) and transcardially perfused with saline and their brains were rapidly removed.

For half of the mice, brains were frozen in isopentane and stored at − 40 °C. Thirteen 20-μm-thick coronal sections were cut at 500 μm interval, from 6.5 to 0.5 mm anterior to the interaural line, according to a stereotaxic brain atlas [24], to evaluate vascular cell adhesion molecule-1 (VCAM-1) expression, hemorrhagic transformations, the MCA vasospasm, cortical lesion, and edema.

For the other half of the mice, brains were sectioned into seven 1-mm-thick coronal slices using the MacIlwain Tissue Chopper (Mickle Laboratory Engineering, Gomshall, Surrey, UK). The cortex located within the core of the lesion (slices three to five) was collected and immediately stored at − 40 °C for the western blotting of BBB proteins and hemoglobin.

Immunohistochemistry for Vascular Cell Adhesion Molecule-1

For each mouse, six coronal brain sections (from 5.5 to 0.5 mm anterior to the interaural line at 1 mm interval) were mounted on the same glass slide and fixed for 10 min in acetone at 4 °C, dried at room temperature, and then rehydrated in PBS 0.1 M pH 7.4. After inhibition of endogenous peroxidase with 0.3% H_2O_2 in PBS-3% methanol for 10 min, sections were incubated with 5% goat serum (S26, Chemicon, Merk Millipore, Saint Quentin en Yvelines, France) for 40 min to block nonspecific immunolabeling. Sections were then incubated overnight at 4 °C with the primary antibody (rat anti-mouse VCAM-1, clone MCA 2297, Serotec, Oxford, UK) diluted 1:200 in PBS-5% goat serum. Sections were then sequentially incubated at room temperature with the second antibody (biotinylated goat anti-rat IgG, STAR 131B, Serotec) diluted 1:400 in PBS-5% goat serum for 2 h and with an avidin-biotin complex solution (VECTASTAIN® Elite ABC kit, PK-6100, Vector Laboratories, Peterborough, UK) for 30 min. Brain sections of ischemic animals in which the primary antibody was omitted were used as negative controls. Staining was visualized using 3,3′-diaminobenzidine tetrahydrochloride (DAB; D5905, Sigma, Saint Quentin Fallavier, France) and digitized (1380 × 1034 pixels/photograph) with a Zeiss Axioskop microscope (Gottingen, Germany). Quantification of VCAM-1 was blindly performed in two regions of interest (ROI) in the ischemic core and the penumbra of each section (Fig. 2a). Analysis was performed with ImageJ processing software (National Institutes of Health, Bethesda, MD, USA). Background was excluded by adjusting the threshold in ImageJ to exclusively highlight the vessels. The total stained vascular surface was obtained by summing the stained surface of the 12 ROI (2 ROI × 6 sections) and was expressed in pixels.

Western Blot Analysis of Endothelial Junction Proteins and Hemoglobin

Brain tissue was processed according to the protocol of [9]. Afterwards, for each sample, proteins (30 μg) were separated on a 6% (VE-cadherin), 12% (claudin-5 and occludin), or 15% (hemoglobin) SDS-polyacrylamide gel and transferred to polyvinylidene difluoride membranes at 100 V for 1 h. Membranes were blocked with 5% non-fat milk in 0.1% TBS-Tween 20 (TBS-T) for 1 h and incubated overnight at 4 °C with the corresponding primary antibody diluted in 5% non-fat milk TBS-T: rabbit anti-occludin (1:150; Invitrogen, 71–1500), rabbit anti-claudin-5 (1:150; Invitrogen, 34–1600), goat anti-VE-cadherin (1:400; Santa Cruz Biotechnology, sc-

6458), and rabbit anti-hemoglobin (1:2000; Abcam, EPR3608). After incubation with a specific secondary fluorescein-linked antibody and then a third antibody with an anti-fluorescent alkaline phosphatase conjugate (for more details, see [9]), membranes were finally incubated with the ECF substrate (GE Healthcare, RPN 5785) according to the manufacturer's instructions. Protein bands were then visualized using the Storm 860 imager (Amersham-Pharmacia Biotech, Orsay, France) and semi-quantification was performed with the ImageQuant software 5.2 (Molecular Dynamics, Foster City, CA, USA). For endothelial junction proteins, results were expressed as arbitrary units (AU) of optical density. Hemoglobin content was converted to blood volume using a standard curve made by addition of known volumes of mouse blood (0, 0.5, 1, 1.5, 2, 2.5 μl) to brain homogenates of exsanguino-perfused naive mice followed by western blotting of hemoglobin as described above. The curve indeed showed a linear relationship between added blood volume and optical density for hemoglobin. Blood volume in each sample was then calculated based on this curve and expressed as microliter of blood per milligram of wet tissue (μl/mg wet tissue).

Hemorrhagic Score

Hemorrhagic transformations were evaluated using a score as previously described [22]. Briefly, on each coronal section, microscopic hemorrhages (defined as blood evident to the eye aided by a magnifying glass (× 2) and given a 1 point score) and macroscopic hemorrhages (defined as blood evident to the naked eye and given a score of 3–4 or 5 according to their size and their blood density) were counted. The microscopic and macroscopic hemorrhagic scores were calculated by adding the respective score of the 13 sections for each mouse. A total hemorrhagic score was then calculated by adding the microscopic and macroscopic hemorrhagic scores.

Morphometric Analysis of the MCA and Vasospasm

MCA vasospasm was evaluated on the coronal section located at 2.5 mm anterior to the interaural line after hematoxylin and eosin staining. The section was scanned (× 200 magnification) using a microscope-mounted camera (Leica, DM4000M, Wetzler, Germany) and the luminal area and thickness of the proximal portion of the left MCA were quantified using ImageJ software [25]. A small luminal area/wall thickness ratio indicates a vasospasm.

Infarct Volume and Brain Swelling

Coronal sections were stained with cresyl violet: infarcted (white) area was measured on each slice using ImageJ software and then multiplied by the ratio of the surface of the infarcted cortex (ipsilateral) to the intact cortex (contralateral) to correct the lesion for brain edema [26]. Infarct volume was calculated by linear integration of infarcted areas in the 13 coronal sections.

Brain swelling, indicating edema, was also calculated according to the following formula: [(ipsilateral cortex volume − contralateral cortex volume)/contralateral cortex volume] × 100.

Statistical Analysis

The data and statistical analysis comply with the recommendations on experimental design and analysis in pharmacology [27]. Median and IQR (first quartile to third quartile) statistics were used for nonparametric measurements, and average and SEM were used for parametric measurements.. Statistical analyses were performed using GraphPad Prism software (GraphPad prism, Prism 5 for Mac, version 5.0). Data of infarct volume, brain edema, MCA vasospasm, and AUC of the CBF curves were analyzed by ANOVA followed by Student *t* test with Bonferroni correction for multiple comparisons. Data of neurological deficit, locomotor activity, western blotting, immunohistochemistry, and hemorrhagic transformations were analyzed by a non-parametric Kruskall-Wallis test with subsequent comparison by Mann-Whitney *U* test with Bonferroni corrections for multiple comparisons. Repeated measures ANOVA followed by Student *t* test with Bonferroni corrections for multiple comparisons were used to evaluate differences in CBF among experimental groups. Differences were statistically significant for a P value < 0.05.

Materials

Alpha-thrombin was purchased from Hematologic Technologies Inc. (Essex Junction, USA). Tissue plasminogen activator (rt-PA) was obtained from Boehringer-Ingelheim, Biberach an der Reiss (Germany). The PARP inhibitor PJ34 and the DAB were both obtained from Sigma-Aldrich (Saint Quentin Fallavier, France). The primary antibodies anti-occludin and anti-claudin-5 were purchased from Invitrogen, ThermoFisher Scientific (Illkirch, France), and the anti-VE-cadherin antibody was purchased from Santa Cruz Biotechnology (Heidelberg, Germany). The primary antibody anti-VCAM-1 and the secondary biotinylated anti-IgG clone were purchased from Serotec (Oxford, UK).

Results

PJ34 Improves Reperfusion After rt-PA Administration

To avoid prolonged anesthesia, we first studied the effect of the single administration of PJ34 given just after thrombin injection (0 h) and showed that it does not alter CBF during

3 h following ischemia onset (i.e., before the second administration of PJ34) compared to saline-treated animals (Fig. 1a). In a second experiment, a total of 22 mice were used and CBF was measured from 3 h after ischemia onset (i.e., the time of the second PJ34 administration) up to 2 h after rt-PA injection. One mouse with spontaneous reperfusion within 30 min after thrombin injection was excluded and one mouse died in the group treated with rt-PA and PJ34 at 3 h. Thrombin injection into the MCA led to an immediate and similar CBF drop in the four groups of mice (Fig. 1b). Administration of PJ34 (once or twice) did not alter CBF within 3 to 4 h after ischemia onset compared to mice receiving saline. Administration of rt-PA at 4 h induced a slow and low reperfusion that did not reach significant statistical level whatever the time point after its injection. However, the AUC calculated between 4 and 6 h post-ischemia onset showed a significant increase in CBF in rt-PA-treated animals compared to saline-treated animals (Fig. 1c). When given twice with rt-PA, PJ34 significantly enhanced CBF compared to rt-PA alone at each time point from 30 min after rt-PA injection. The AUC of this association was also significantly increased compared to rt-PA alone. Although the single administration of PJ34 at 3 h did not significantly increase reperfusion compared to the rt-PA-treated group at individual time points, this protocol

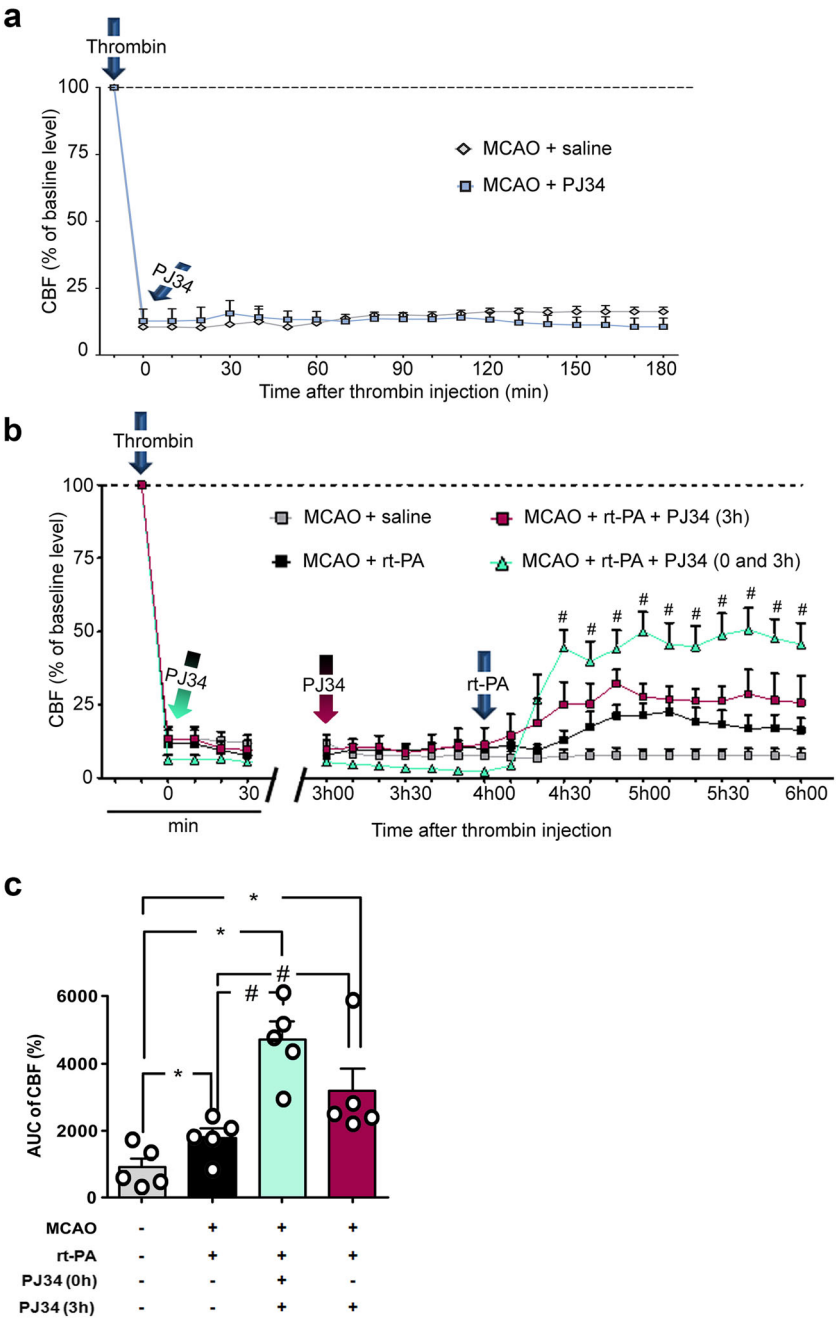

Fig. 1 Effect of PJ34 on reperfusion after MCA occlusion (MCAO). **a** Early PJ34 administration just after thrombin injection did not modify the cerebral blood flow (CBF) after MCAO. CBF was recorded above the core of the MCA territory for 3 h after MCAO in mice receiving PJ34 (3 mg kg^{-1}) or saline intraperitoneally. The arrows indicate the time point of thrombin injection in the MCA and the injection of PJ34. Data are mean ± SEM ($n = 5$ per group). **b** PJ34 improved rt-PA-induced reperfusion after MCAO. The arrows indicate the time point of thrombin injection in MCA, rt-PA (0.9 mg kg^{-1}) intravenous injection, and PJ34 administration. When given twice with rt-PA, PJ34 (3 mg kg^{-1}) significantly enhanced CBF compared to rt-PA-treated mice. **c** Area under the curve (AUC) was calculated by measuring the area under the CBF curve between the injection of rt-PA (4 h) and the end of CBF monitoring (6 h). Data are mean ± SEM ($n = 5$ per group). $^{*}P < 0.05$ versus MCAO + saline; $^{\#}P < 0.05$ versus MCAO + rt-PA

significantly improved rt-PA-induced reperfusion evaluated by the AUC.

Effect of rt-PA and PJ34 on Post-Ischemic Outcomes

A total of 135 mice were used in this experiment; exclusion, mortality, and CBF drop are given in Table 1.

Association of PJ34 with rt-PA Reduces Vascular Inflammation

VCAM-1 expression was evaluated in the ischemic core and penumbra by immunochemistry (Fig. 2a, b). Cerebral ischemia led to a massive increase in VCAM-1 expression in both ROI at 24 h after cerebral ischemia as compared to sham-operated mice (Fig. 2c, d). The total expression of VCAM-1 was also increased by ischemia (Fig. 2e). Administration of rt-PA or PJ34 alone did not modify the post-ischemic expression of VCAM-1 whatever the ROI. The association of PJ34 (given 3 h post-ischemia) with rt-PA led to a marked reduction in post-ischemic total and penumbra VCAM-1 expression as compared to saline-treated ischemic mice.

Association of PJ34 with rt-PA Reduces Hemorrhagic Transformations and Endothelial Junction Protein Degradation

Hemorrhagic transformations were first evaluated through a hemorrhagic score (Fig. 3a–d). Ischemia significantly increased the total hemorrhagic score compared to sham-operated mice (Fig. 3a). The post-ischemic total hemorrhagic score was not modified by PJ34 alone. By contrast, rt-PA induced a threefold increase in the total hemorrhagic score of ischemic mice. Combining PJ34 with rt-PA suppressed rt-PA-induced hemorrhages, whether PJ34 was administered twice or just once at 3 h. Of note, the effect of PJ34 was similar on both macroscopic and microscopic hemorrhages (Fig. 3b, c). To confirm the anti-hemorrhagic effect of PJ34 against rt-PA, cortical blood content was detected by Western blotting of hemoglobin (Fig. 3e, f). The level of blood in the ipsilateral cortex of saline-treated ischemic mice was significantly increased compared to that of sham-operated mice (Fig. 3f). PJ34 did not modify the amount of cortical blood in ischemic mice while rt-PA increased this amount. In rt-PA-treated ischemic mice, PJ34 significantly reduced the blood content by 70% when administered twice and by 55% after a single administration at 3 h.

As increased blood-brain barrier permeability may account for hemorrhagic transformations, we next examined expression of tight junction proteins, including transmembrane claudin-5 and occludin, and the adherens junction protein VE-cadherin. Twenty-four hours after ischemia, the expression of these three junction proteins was not modified compared to sham-operated mice (Fig. 3g–i). PJ34 alone had no effect on the expression of junction proteins in ischemic mice compared to those treated with saline. Delayed rt-PA administration significantly decreased by half the expression of occludin, claudin-5, and VE-cadherin in ischemic mice. The administration of PJ34, even when delayed 3 h post-ischemia, prevented the degradation of these proteins by rt-PA.

Association of PJ34 with rt-PA Reduces MCA Vasospasm

MCA vasospasm was evaluated by the luminal area/wall thickness ratio (the lower the ratio, the more severe the vasospasm).

The luminal area in the ischemic mice was significantly reduced as compared to sham-operated mice (1042 ± 302.5 μm^2 versus 3276 ± 505.3 μm^2; $P < 0.05$). PJ34 and rt-PA were devoid of any effect when administered alone. By contrast, the association of PJ34 with rt-PA increased the luminal area of the MCA as compared to the rt-PA-treated group by 101% ($P < 0.05$) when PJ34 was injected twice and by 155% ($P < 0.05$) when it was administered once 3 h after ischemia onset (data not shown). The wall thickness of the MCA was significantly increased in the saline-treated ischemic mice as compared with the sham-operated mice (25.7 ± 2.77 μm versus 14.3 ± 1.47 μm; $P < 0.05$). PJ34 and rt-PA were devoid of any effect when administered alone. The

Table 1 Effect of rt-PA and PJ34 on post-ischemic outcomes: distribution of ischemic animals

Total of animals	$n = 135$	
Excluded animals		
CBF drop < 50%	$n = 2$	
Spontaneous reperfusion	$n = 7$	
Groups	Number of mice (dead − included)	Residual blood flow (%)
Ischemia + saline	6/26–20	6 ± 1
Ischemia + rt-PA	8/27–19	5 ± 1
Ischemia + PJ34	6/25–19	7 ± 1
Ischemia + rt-PA + PJ34 (0 and 3 h)	4/23–19	9 ± 1
Ischemia + rt-PA + PJ34 (3 h)	5/25–20	9 ± 1

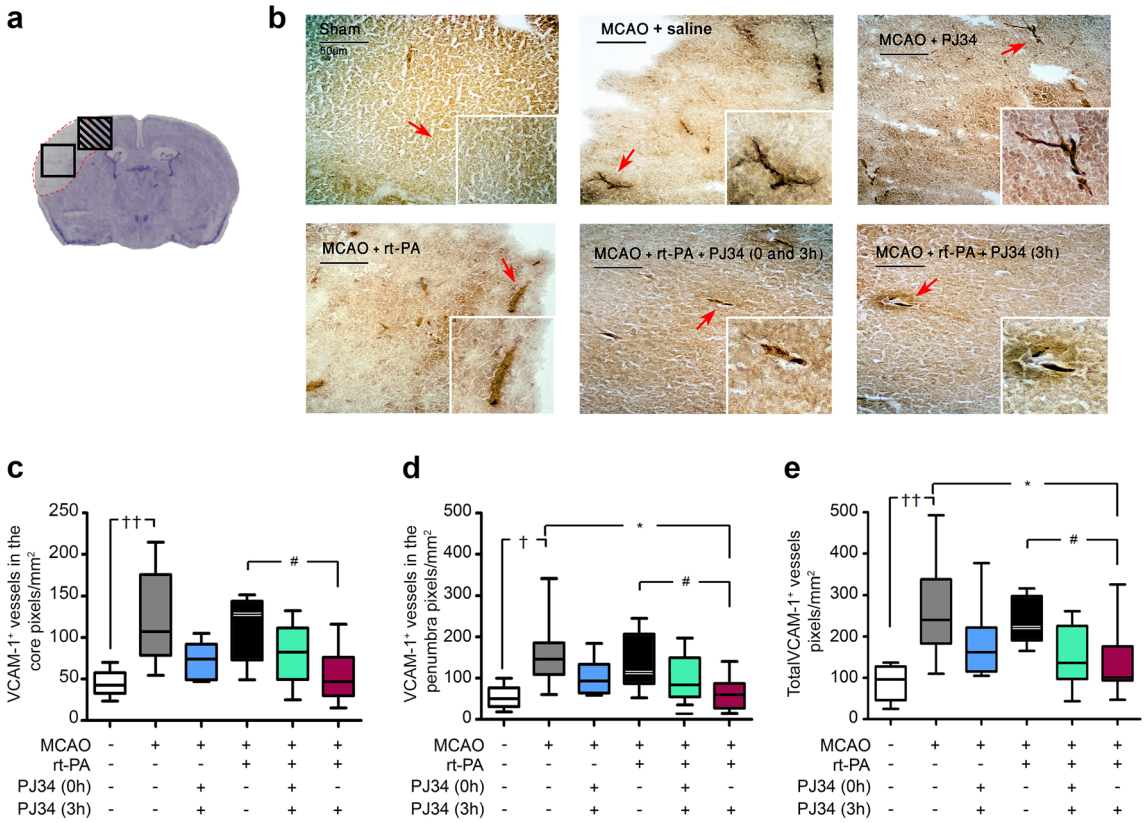

Fig. 2 Effect of PJ34 and rt-PA on VCAM-1 expression 24 h after MCA occlusion (MCAO). **a** Regions of interest (ROI) for VCAM-1 immunohistochemistry. Representative cresyl violet-stained coronal slice showing the brain lesion (in white) and the location of ROI in the ischemic core (white square) and in the penumbra (hatched square). **b** Representative VCAM-1 immunostaining in the cerebral cortex of each group. Scale bar represents 50 µm. **c**–**e** Quantification showing increased expression of VCAM-1 in the cerebral cortex after ischemia. The expression of VCAM-1 was reduced by the combined PJ34 (3 mg kg^{-1}) and rt-PA (0.9 mg kg^{-1}) treatment. $^{\dagger}P<0.05$, $^{\dagger\dagger}P<0.01$ versus sham; $^{*}P<0.05$ versus MCAO + saline; $^{\#}P<0.05$ versus MCAO + rt-PA ($n=9$–10 per group)

association of rt-PA and PJ34 reduced the MCA wall thickness as compared to the rt-PA treated ischemic mice by 47% ($P<0.05$) when PJ34 was injected twice and by 32% ($P<0.05$) when it was administered once 3 h after ischemia onset (data not shown).

The luminal area/wall thickness ratio was significantly reduced after ischemia compared to sham-operated mice indicating MCA vasospasm (Fig. 4). This vasospasm was modified neither by PJ34 nor by rt-PA alone. By contrast, the association of both compounds reduced MCA vasospasm even when injection of PJ34 was delayed 3 h after ischemia onset.

Association of PJ34 with rt-PA Reduces the Cortical Lesion and Edema

Ischemia induced a cortical infarction that was modified neither by PJ34 nor by rt-PA alone (Fig. 5a, b). Combined treatment of rt-PA with PJ34, administered twice or once, reduced by 70% brain infarction compared to the rt-PA and saline groups.

Ischemia led to an ipsilateral cortical swelling (≈ + 10% as compared to the contralateral cortex; Fig. 5c). Neither the administration of PJ34 alone nor that of rt-PA had any effect on cortical swelling. By contrast, the association of both compounds reduced by 66 and 55% ischemia-induced cortical edema, depending on whether mice received both or only one administration of PJ34, respectively.

Association of PJ34 with rt-PA Improves Functional Outcomes

The locomotor activity was not significantly different in sham-operated and ischemic mice treated with saline (Fig. 5d). PJ34 per se had no effect, while rt-PA reduced the locomotor activity of ischemic mice by 49% compared to the saline-treated group (157 ± 29 versus 307 ± 48 counts/60 min). The combination of PJ34, administered at 0 and 3 h post-ischemia, with rt-PA suppressed the locomotor hypoactivity induced by rt-PA (329 ± 56 counts/60 min).

Ischemia induced a significant neurological deficit at 24 h compared to sham-operated mice (4.5 ± 0.3 versus 7.7 ± 0.1) that was modified neither by PJ34 nor by rt-PA alone (Fig. 5e). In ischemic mice, the association of both treatments significantly improved the neurological score compared to rt-PA alone, whether PJ34 was administered twice or once (6.4 ±

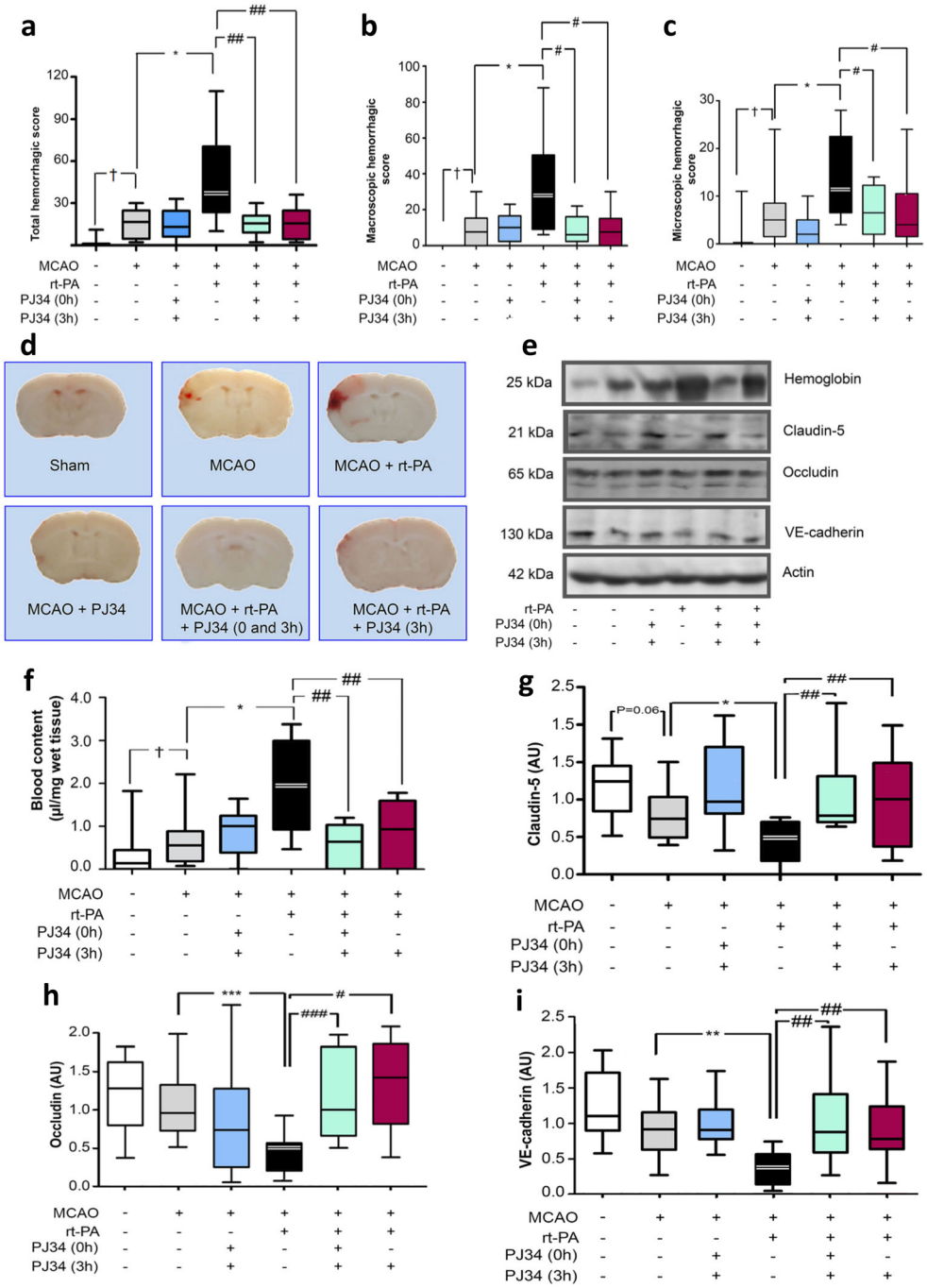

Fig. 3 Effect of PJ34 and rt-PA on hemorrhagic transformations and blood-brain barrier junction proteins after MCA occlusion (MCAO). **a**–**c** Quantification of hemorrhagic score demonstrated a significant increase in total (**a**), macroscopic (**b**), and microscopic (**c**) hemorrhages after MCAO that was significantly aggravated by rt-PA administration. The combined treatment with PJ34 provided significant protection against rt-PA-induced hemorrhagic transformations. **d** Representative brain sections (bregma − 0.10 mm) for visual hemorrhage examination. **e** Representative blots of Western blot of hemoglobin (25 kDa), claudin-5 (21 kDa), occludin (65 kDa) and VE-cadherin (130 kDa). **f** The blood content was increased after rt-PA administration and the association of PJ34 to rt-PA prevented this increase. **g**–**i** PJ34 protects the junction proteins claudin-5 (**g**), occludin (**h**) and VE-cadherin (**i**) from the degradation induced by rt-PA in ischemic mice. $^{\dagger}P < 0.05$ versus sham; $^{*}P < 0.05$, $^{**}P < 0.01$, and $^{***}P < 0.001$ versus saline; $^{\#}P < 0.05$, $^{\#\#}P < 0.01$, $^{\#\#\#}P < 0.001$ versus rt-PA ($n = 9$–10 for each group)

0.3 and 6.1 ± 0.2 versus 3.6 ± 0.3, respectively), but also compared to the saline group.

Discussion

The present study shows for the first time that the PARP inhibitor PJ34 improves rt-PA-induced reperfusion, acts synergistically with rt-PA to decrease post-ischemic vascular inflammation and MCA vasospasm, and decreased rt-PA-induced BBB disruption and hemorrhagic transformations in a thromboembolic model of ischemic stroke. Together, PJ34 and rt-PA also reduced brain edema, infarct volume, and neurological deficit with an extended therapeutic window compared to rt-PA alone.

Delayed rt-PA administration in our thromboembolic model of cerebral ischemia led to a low reperfusion rate that might be due to increased clot resistance to fibrinolysis over time and/or to the "no-reflow" phenomenon [18]. This effect is similar to the clinical situation after stroke since clinical data

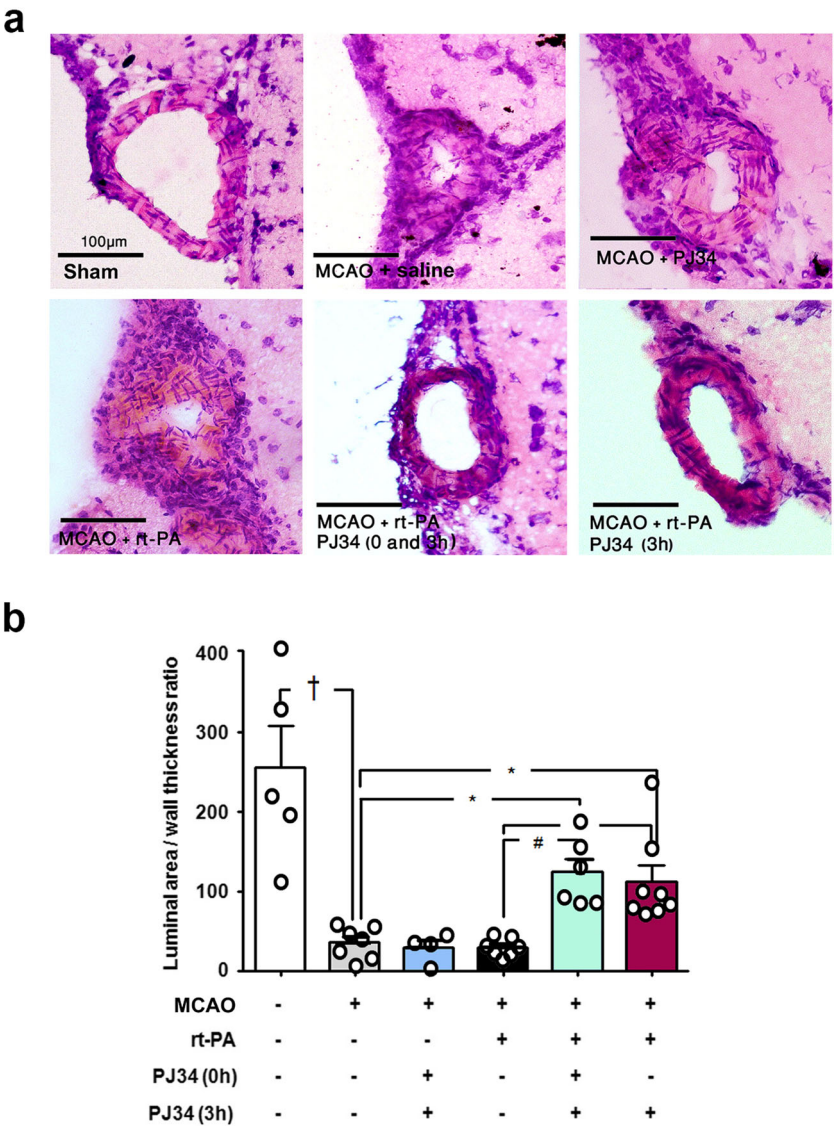

Fig. 4 Effect of PJ34 and rt-PA on MCA vasospasm 24 h after MCA occlusion (MCAO). **a** Representative pictures of MCA vasospasm. Scale bar represents 100 µm. **b** Quantification showing a decreased luminal area/wall thickness ratio in the MCA after ischemia and rt-PA (0.9 mg kg^{-1}) administration. The association of PJ34 (3 mg kg^{-1}) and rt-PA protected the MCA against vasospasm. Data are mean ± SEM ($n = 9$–10 per group). $^{\dagger}P < 0.05$ versus sham; $^{*}P < 0.05$ versus MCAO + saline; $^{\#}P < 0.05$ versus MCAO + rt-PA

shows that in proximal middle cerebral artery occlusions, reperfusion with intravenous rt-PA is achieved in less than 20% of patients [28–30]. We show herein that PJ34 improves reperfusion in the first hours after rt-PA treatment. Although no interference with rt-PA thrombolysis was reported in vitro for INO-1001, another PARP inhibitor, or minocycline, a tetracycline described as a potent PARP inhibitor [31–33], we cannot exclude that PJ34 potentiates thrombolysis in our conditions and/or increases the clot sensitivity to rt-PA. Finally, PJ34 might act through mechanism(s) independent from thrombolysis to increase reperfusion (e.g., we previously reported that PJ34 possesses antiaggregant activity on human platelet [34]).

PARP has been implicated in endothelial dysfunction in various diseases such as atherosclerosis, hypertension, diabetes, chronic heart failure, and aging [35]. In particular, PARP participates to vascular inflammation through interactions with transcription factors such as NF-κB [36] and Bcl6 [37], an inducer and a repressor of inflammatory genes, respectively. Thus, PARP regulates the expression of cytokines and cell adhesion molecules [38]. Among the latest, the integrin ICAM-1 and selectins (E- and P-selectins) have already been the subject of numerous stroke studies [39], while interest in VCAM-1 is more recent. VCAM-1, an endothelial cell ligand for α4β1 or α4β7 integrins expressed on various blood leukocytes, is of particular interest as it is not constitutively expressed but has been reported to be upregulated specifically on activated vascular endothelial cells after stroke [40]. Increased VCAM-1 expression was also found in infarcted areas of autopsy specimens from patients with recent stroke [41] and in the plasma of stroke patients [42]. In our model, VCAM-1 protein is upregulated 24 h after ischemia. Changes in VCAM-1 after rt-PA were only examined in two studies that reported an increase in VCAM-1 mRNA amounts either 24 or 72 h after cerebral ischemia [43]. In the present work, rt-PA did not potentiate the post-ischemic increase in VCAM-1 at the protein level. PJ34 reduced VCAM-1 protein

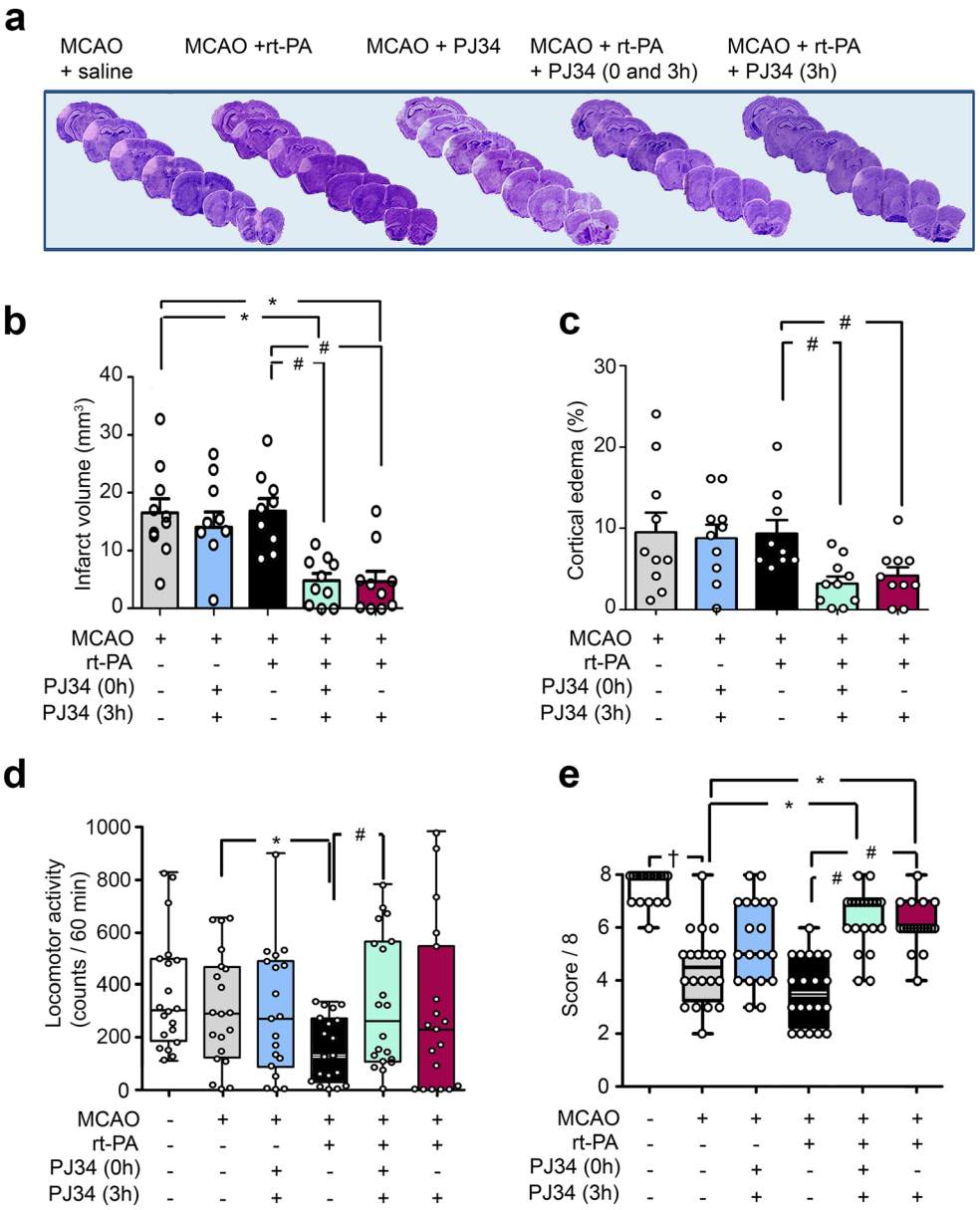

Fig. 5 Effect of PJ34 and rt-PA on cortical lesion, edema, and functional outcomes 24 h after cerebral ischemia. **a** Representative brain lesions, stained with cresyl violet, for each ischemic group. **b** Quantification of cortical lesion and **c** edema after rt-PA (0.9 mg kg^{-1}) administration and treatment with PJ34 (3 mg kg^{-1}). A significantly reduced infarct volume and edema were observed in mice treated with PJ34 and rt-PA (n = 9–10 for each group). **d** Locomotor activity. rt-PA administration after cerebral ischemia-induced hypoactivity. The combination of PJ34 (3 mg kg^{-1}) to rt-PA (0.9 mg kg^{-1}) restored locomotor activity. **e** Neurological score. The combined administration of PJ34 and rt-PA improved the neurological score after cerebral ischemia.(**d**, **e**: n = 19–20 per group). $^{\dagger}P < 0.05$ versus sham; $^{*}P < 0.05$ versus MCAO + saline; $^{\#}P < 0.05$ versus MCAO + rt-PA

in the brain of rt-PA-treated ischemic animals. The role of VCAM-1 in experimental stroke remains controversial: one study using antibodies directed against VCAM-1 showed no neuroprotection, while VCAM-1 gene silencing by in vivo small interfering RNA injection reduced post-ischemic neuroinflammation and brain infarction in another study performed in permanent and transient cerebral ischemia [44]. However, in clinical studies, VCAM-1 has been demonstrated to be a marker of clinical outcome after acute cerebral ischemia [45] and has been suggested to be predictive of recurrent strokes [42]. Next, we examined whether reduction of endothelial inflammation by combining PJ34 with rt-PA was associated with other beneficial vascular effects.

PJ34 reduced the degradation of tight junction (claudin-5, occludin) and adherens junction (VE-cadherin) proteins that might contribute to the reduction in the aggravation of hemorrhagic transformations induced by rt-PA in our thromboembolic stroke model. Reduction of junction protein degradation might also contribute to decrease edema observed when PJ34 is associated with rt-PA.

Reduced endothelial vasoreactivity was reported after cerebral ischemia/reperfusion and could contribute to impaired blood flow restoration [46]. Post-ischemic vasoconstriction of MCA was also observed; the underlying proposed mechanisms include decreased availability of nitric oxide and impaired vasodilatation, upregulation of vasoconstrictor receptors (endothelin-1, angiotensin-1, and 5HT1B receptors), or spreading depolarization and vascular inflammation [47]. Treatment with rt-PA was demonstrated to further impair myogenic tone and reactivity of MCA after cerebral ischemia in rats and to reduce the sensitivity of the

cerebral artery to acetylcholine induced-vasodilatation [48]. Impairment of hypercapnia and hypotensive cerebrovasodilation was also reported after rt-PA treatment in pial arteries of newborn pig submitted to cerebral ischemia [49]. Our results show that, in our model, cerebral ischemia induces MCA vasospasm that is not potentiated by rt-PA. The drastic reduction in MCA diameter by ischemia per se could render impossible the aggravation by rt-PA. PARP inhibitors were reported to improve endothelium-dependent relaxation in hypertensive and diabetic animals [50]. Interactions either downstream or upstream the vasoconstrictor mediator endothelin-1 and the renin-angiotensin aldosterone system were also reported for PARP inhibitors in peripheral endothelium [51]. Furthermore, PARP inhibition has been demonstrated to reduce cerebral vasospasm after subarachnoid hemorrhage [52]. Taken together, these studies led us to investigate the effect of PJ34 on MCA vasospasm after cerebral ischemia. PJ34 was devoid of effect per se but when combined with rt-PA, it increased MCA lumen and reduced MCA wall thickness. It remains to be established whether this effect (1) improves blood supply downstream to brain parenchyma and finally contributes to neuroprotection or (2) is a consequence of less damaged neurons with PJ34 and rt-PA treatment and thus an increased need for blood supply. Interestingly, even though the cause of MCA vasospasm reduction by PJ34 is unknown, these data support our findings that combining PJ34 with rt-PA improves the post-ischemic reperfusion and protects against the vascular dysfunction.

As we did not measure cardiac output and arterial blood pressure, we cannot exclude that some of the beneficial effects of PJ34 on reperfusion could be related to its favorable influence on the peripheral circulation. However, on the basis of previous results, it appears that inhibition of PARP-1 activity does not alter the systolic arterial pressure [53–55] but improves microvascular function through restoration of the endothelial NO synthase phosphorylation pathway [54].

Taken together, our data clearly highlight the implication of PARP in rt-PA vascular toxicity after stroke.

In terms of neuroprotection, we show that associating PJ34 with delayed rt-PA reduces brain infarction. This effect shown by using the thromboembolic model of cerebral ischemia could not be detected in the severe model of mechanical and permanent MCA occlusion where thrombolysis could not be achieved [9]. Indeed, this effect could result from the better reperfusion because the combined therapy increased reperfusion to about 50% of baseline level, a value defined as a threshold for neuronal death [56]. Furthermore, this improved reperfusion is of major interest as it is has been suggested that neuroprotective therapies could fail in humans because the damaged vascular network is unable to deliver the necessary nutrients and treatment to the tissue at risk, thus also hampering neuroprotection [3].

To evaluate the overall benefit of vascular and neuronal protection elicited by combining rt-PA and PJ34, a functional examination of mice including locomotor activity and sensorimotor tests was performed. Delayed rt-PA administration 4 h after ischemia onset decreased the locomotor activity which is in line with other studies using intraluminal MCA occlusion model [57, 58]. Our treatment with PJ34, given either once or twice, was able to counteract this detrimental effect of rt-PA. Sensorimotor tests also demonstrated neurological improvement by combining PJ34 with rt-PA. In the present study, we show the multifaceted vascular benefit and neuroprotection of combining PJ34 with rt-PA and further studies are required to elucidate whether this combination improves the long-term functional recovery after stroke.

Conclusion

In summary, our study is the first showing the multifaceted vasculoprotection achieved by PJ34 that acts synergistically with rt-PA to improve reperfusion and reduce vasospasm and vascular inflammation in the thromboembolic model of cerebral ischemia. The association of both compounds leads to a “safe” thrombolysis and neurological improvement with an extended therapeutic window for rt-PA after stroke. These results are especially encouraging given that in the last 3 years, the US Food and Drug Administration and European Medicines Agency approved the use of several PARP inhibitor for the treatment of different cancers [59, 60] .

Authors' Contributions DL, MEA, and IM conceived and designed the experiments. MEA, MG, BB, and CA performed the experiments. MEA, DL, BP, and BC analyzed the data. MEA, DL, VBB, CML, and IM wrote the manuscript.

Funding Information M. El-Amki and. M. Garraud are recipients of a Ph.D. grant from the Université Paris Descartes, Université Sorbonne Paris Cité.

Compliance with Ethical Standards

All experiments were performed on male Swiss albino mice (25–32 g, Janvier, Le Genest-St-Isle, France) in compliance with the European Community Council Directive of September 22, 2010 (2010/63/UE), and the French regulations regarding the protection of animals used for experimental and other scientific purposes (D2013-118), with the ethical approval of the Paris Descartes University Animal Ethics Committee (registered number P2.CM.152.10).

Conflict of Interest The authors declare that they have no conflicts of interest.

References

1. Cronin CA (2010) Intravenous tissue plasminogen activator for stroke: a review of the ECASS III results in relation to prior clinical

trials. J Emerg Med 38:99–105. https://doi.org/10.1016/j.jemermed.2009.08.004
2. Tsivgoulis G, Sharma VK, Mikulik R, Krogias C, Haršány M, Shahripour RB, Athanasiadis D, Teoh HL et al (2014) Intravenous thrombolysis for acute ischemic stroke occurring during hospitalization for transient ischemic attack. Int J Stroke 9:413–418. https://doi.org/10.1111/ijs.12125
3. El Amki M, Wegener S (2017) Improving cerebral blood flow after arterial recanalization: a novel therapeutic strategy in stroke. Int J Mol Sci 18. https://doi.org/10.3390/ijms18122669
4. Hacke W, Kaste M, Bluhmki E, Brozman M, Dávalos A, Guidetti D, Larrue V, Lees KR et al (2008) Thrombolysis with alteplase 3 to 4.5 hours after acute ischemic stroke. N Engl J Med 359:1317–1329. https://doi.org/10.1056/NEJMoa0804656
5. Sussman ES, Connolly ES (2013) Hemorrhagic transformation: a review of the rate of hemorrhage in the major clinical trials of acute ischemic stroke. Front Neurol 4:69. https://doi.org/10.3389/fneur.2013.00069
6. Bürkle A, Virág L (2013) Poly(ADP-ribose): PARadigms and PARadoxes. Mol Asp Med 34:1046–1065. https://doi.org/10.1016/j.mam.2012.12.010
7. Ray Chaudhuri A, Nussenzweig A (2017) The multifaceted roles of PARP1 in DNA repair and chromatin remodelling. Nat Rev Mol Cell Biol 18:610–621. https://doi.org/10.1038/nrm.2017.53
8. Haddad M, Beray-Berthat V, Coqueran B, Plotkine M, Marchand-Leroux C, Margaill I (2013) Combined therapy with PJ34, a poly(ADP-ribose)polymerase inhibitor, reduces tissue plasminogen activator-induced hemorrhagic transformations in cerebral ischemia in mice. Fundam Clin Pharmacol 27:393–401. https://doi.org/10.1111/j.1472-8206.2012.01036.x
9. Teng F, Beray-Berthat V, Coqueran B, Lesbats C, Kuntz M, Palmier B, Garraud M, Bedfert C et al (2013) Prevention of rt-PA induced blood-brain barrier component degradation by the poly(ADP-ribose)polymerase inhibitor PJ34 after ischemic stroke in mice. Exp Neurol 248:416–428. https://doi.org/10.1016/j.expneurol.2013.07.007
10. Kim Y, Kim YS, Kim HY, Noh MY, Kim JY, Lee YJ, Kim J, Park J et al (2018) Early treatment with poly(ADP-ribose) polymerase-1 inhibitor (JPI-289) reduces infarct volume and improves long-term behavior in an animal model of ischemic stroke. Mol Neurobiol. https://doi.org/10.1007/s12035-018-0910-6
11. Matsuura S, Egi Y, Yuki S, Horikawa T, Satoh H, Akira T (2011) MP-124, a novel poly(ADP-ribose) polymerase-1 (PARP-1) inhibitor, ameliorates ischemic brain damage in a non-human primate model. Brain Res 1410:122–131. https://doi.org/10.1016/j.brainres.2011.05.069
12. Giansanti V, Donà F, Tillhon M, Scovassi AI (2010) PARP inhibitors: new tools to protect from inflammation. Biochem Pharmacol 80:1869–1877. https://doi.org/10.1016/j.bcp.2010.04.022
13. Haddad M, Rhinn H, Bloquel C, Coqueran B, Szabó C, Plotkine M, Scherman D, Margaill I (2006) Anti-inflammatory effects of PJ34, a poly(ADP-ribose) polymerase inhibitor, in transient focal cerebral ischemia in mice. Br J Pharmacol 149:23–30. https://doi.org/10.1038/sj.bjp.0706837
14. Crome O, Doeppner TR, Schwarting S, Müller B, Bähr M, Weise J (2007) Enhanced poly(ADP-ribose) polymerase-1 activation contributes to recombinant tissue plasminogen activator-induced aggravation of ischemic brain injury in vivo. J Neurosci Res 85:1734–1743. https://doi.org/10.1002/jnr.21305
15. Kauppinen TM, Suh SW, Berman AE, Hamby AM, Swanson RA (2009) Inhibition of poly(ADP-ribose) polymerase suppresses inflammation and promotes recovery after ischemic injury. J Cereb Blood Flow Metab 29:820–829. https://doi.org/10.1038/jcbfm.2009.9
16. Moroni F, Cozzi A, Chiarugi A, Formentini L, Camaioni E, Pellegrini-Giampietro DE, Chen Y, Liang S et al (2012) Long-lasting neuroprotection and neurological improvement in stroke models with new, potent and brain permeable inhibitors of poly(ADP-ribose) polymerase. Br J Pharmacol 165:1487–1500. https://doi.org/10.1111/j.1476-5381.2011.01666.x
17. Berger NA, Besson VC, Boulares AH, Bürkle A, Chiarugi A, Clark RS, Curtin NJ, Cuzzocrea S et al (2017) Opportunities for the repurposing of PARP inhibitors for the therapy of non-oncological diseases. Br J Pharmacol 175:192–222. https://doi.org/10.1111/bph.13748
18. El Amki M, Lerouet D, Coqueran B et al (2012) Experimental modeling of recombinant tissue plasminogen activator effects after ischemic stroke. Exp Neurol 238:138–144. https://doi.org/10.1016/j.expneurol.2012.08.005
19. Cossu G, Messerer M, Oddo M, Daniel RT (2014) To look beyond vasospasm in aneurysmal subarachnoid haemorrhage. Biomed Res Int 2014:628597. https://doi.org/10.1155/2014/628597
20. Orset C, Macrez R, Young AR, Panthou D, Angles-Cano E, Maubert E, Agin V, Vivien D (2007) Mouse model of in situ thromboembolic stroke and reperfusion. Stroke 38:2771–2778. https://doi.org/10.1161/STROKEAHA.107.487520
21. Astrup J, Symon L, Branston NM, Lassen NA (1977) Cortical evoked potential and extracellular K+ and H+ at critical levels of brain ischemia. Stroke 8:51–57
22. Haddad M, Beray-Berthat V, Coqueran B, Palmier B, Szabo C, Plotkine M, Margaill I (2008) Reduction of hemorrhagic transformation by PJ34, a poly(ADP-ribose)polymerase inhibitor, after permanent focal cerebral ischemia in mice. Eur J Pharmacol 588:52–57. https://doi.org/10.1016/j.ejphar.2008.04.013
23. Homsi S, Piaggio T, Croci N, Noble F, Plotkine M, Marchand-Leroux C, Jafarian-Tehrani M (2010) Blockade of acute microglial activation by minocycline promotes neuroprotection and reduces locomotor hyperactivity after closed head injury in mice: a twelve-week follow-up study. J Neurotrauma 27:911–921. https://doi.org/10.1089/neu.2009.1223
24. Paxinos G, Franklin KBJ (1997) The mouse brain in stereotaxic coordinates / George Paxinos, Keith B.J. Franklin. Academic, San Diego, Calif. ; London :
25. Sabri M, Ai J, Macdonald RL (2011) Dissociation of vasospasm and secondary effects of experimental subarachnoid hemorrhage by clazosentan. Stroke 42:1454–1460. https://doi.org/10.1161/STROKEAHA.110.604728
26. Golanov EV, Reis DJ (1995) Contribution of cerebral edema to the neuronal salvage elicited by stimulation of cerebellar fastigial nucleus after occlusion of the middle cerebral artery in rat. J Cereb Blood Flow Metab 15:172–174. https://doi.org/10.1038/jcbfm.1995.19
27. Curtis MJ, Bond RA, Spina D, Ahluwalia A, Alexander SPA, Giembycz MA, Gilchrist A, Hoyer D et al (2015) Experimental design and analysis and their reporting: new guidance for publication in BJP. Br J Pharmacol 172:3461–3471. https://doi.org/10.1111/bph.12856
28. Rubiera M, Alvarez-Sabín J, Ribo M et al (2005) Predictors of early arterial reocclusion after tissue plasminogen activator-induced recanalization in acute ischemic stroke. Stroke 36:1452–1456. https://doi.org/10.1161/01.STR.0000170711.43405.81
29. Bhatia R, Hill MD, Shobha N, Menon B, Bal S, Kochar P, Watson T, Goyal M et al (2010) Low rates of acute recanalization with intravenous recombinant tissue plasminogen activator in ischemic stroke: real-world experience and a call for action. Stroke 41:2254–2258. https://doi.org/10.1161/STROKEAHA.110.592535
30. Meschia JF, Barrett KM, Brott TG (2013) Reperfusion therapy for acute ischemic stroke: how should we react to the Third Interventional Management of Stroke (IMS III) trial? Mayo Clin Proc 88:653–657. https://doi.org/10.1016/j.mayocp.2013.05.002
31. Alano CC, Kauppinen TM, Valls AV, Swanson RA (2006) Minocycline inhibits poly(ADP-ribose) polymerase-1 at nanomolar

concentrations. Proc Natl Acad Sci U S A 103:9685–9690. https://doi.org/10.1073/pnas.0600554103
32. Machado LS, Sazonova IY, Kozak A, Wiley DC, el-Remessy AB, Ergul A, Hess DC, Waller JL et al (2009) Minocycline and tissue-type plasminogen activator for stroke: assessment of interaction potential. Stroke 40:3028–3033. https://doi.org/10.1161/STROKEAHA.109.556852
33. Tóth O, Szabó C, Kecskés M, Pótó L, Nagy Á, Losonczy H (2006) In vitro effect of the potent poly(ADP-ribose) polymerase (PARP) inhibitor INO-1001 alone and in combination with aspirin, eptifibatide, tirofiban, enoxaparin or alteplase on haemostatic parameters. Life Sci 79:317–323. https://doi.org/10.1016/j.lfs.2006.01.007
34. Lechaftois M, Dreano E, Palmier B, Margaill I, Marchand-Leroux C, Bachelot-Loza C, Lerouet D (2014) Another "string to the bow" of PJ34, a potent poly(ADP-ribose)polymerase inhibitor: an anti-platelet effect through P2Y12 antagonism? PLoS One 9:e110776. https://doi.org/10.1371/journal.pone.0110776
35. Pacher P, Szabó C (2007) Role of poly(ADP-ribose) polymerase 1 (PARP-1) in cardiovascular diseases: the therapeutic potential of PARP inhibitors. Cardiovasc Drug Rev 25:235–260. https://doi.org/10.1111/j.1527-3466.2007.00018.x
36. Kassan M, Choi S-K, Galán M et al (2013) Enhanced NF-κB activity impairs vascular function through PARP-1-, SP-1-, and COX-2-dependent mechanisms in type 2 diabetes. Diabetes 62:2078–2087. https://doi.org/10.2337/db12-1374
37. Gongol B, Marin T, Peng I-C, Woo B, Martin M, King S, Sun W, Johnson DA et al (2013) AMPKα2 exerts its anti-inflammatory effects through PARP-1 and Bcl-6. Proc Natl Acad Sci U S A 110:3161–3166. https://doi.org/10.1073/pnas.1222051110
38. Rom S, Zuluaga-Ramirez V, Dykstra H, Reichenbach NL, Ramirez SH, Persidsky Y (2015) Poly(ADP-ribose) polymerase-1 inhibition in brain endothelium protects the blood-brain barrier under physiologic and neuroinflammatory conditions. J Cereb Blood Flow Metab 35:28–36. https://doi.org/10.1038/jcbfm.2014.167
39. Frijns CJM, Kappelle LJ (2002) Inflammatory cell adhesion molecules in ischemic cerebrovascular disease. Stroke 33:2115–2122
40. Gauberti M, Montagne A, Quenault A, Vivien D (2014) Molecular magnetic resonance imaging of brain-immune interactions. Front Cell Neurosci 8:389. https://doi.org/10.3389/fncel.2014.00389
41. Krupinski J, Kaluza J, Kumar P, Kumar S, Wang JM (1994) Role of angiogenesis in patients with cerebral ischemic stroke. Stroke 25:1794–1798
42. Castillo J, Alvarez-Sabín J, Martínez-Vila E et al (2009) Inflammation markers and prediction of post-stroke vascular disease recurrence: the MITICO study. J Neurol 256:217–224. https://doi.org/10.1007/s00415-009-0058-4
43. Lenglet S, Montecucco F, Denes A, Coutts G, Pinteaux E, Mach F, Schaller K, Gasche Y et al (2014) Recombinant tissue plasminogen activator enhances microglial cell recruitment after stroke in mice. J Cereb Blood Flow Metab 34:802–812. https://doi.org/10.1038/jcbfm.2014.9
44. Liesz A, Zhou W, Mracskó É, Karcher S, Bauer H, Schwarting S, Sun L, Bruder D et al (2011) Inhibition of lymphocyte trafficking shields the brain against deleterious neuroinflammation after stroke. Brain 134:704–720. https://doi.org/10.1093/brain/awr008
45. Blum A, Khazim K, Merei M, Peleg A, Blum N, Vaispapir V (2006) The stroke trial—can we predict clinical outcome of patients with ischemic stroke by measuring soluble cell adhesion molecules (CAM)? Eur Cytokine Netw 17:295–298
46. Palomares SM, Cipolla MJ (2011) Vascular protection following cerebral ischemia and reperfusion. J Neurol Neurophysiol 2011
47. Edvinsson LIH, Povlsen GK (2011) Vascular plasticity in cerebrovascular disorders. J Cereb Blood Flow Metab 31:1554–1571. https://doi.org/10.1038/jcbfm.2011.70
48. Cipolla MJ, Lessov N, Clark WM, Haley EC (2000) Postischemic attenuation of cerebral artery reactivity is increased in the presence of tissue plasminogen activator. Stroke 31:940–945
49. Armstead WM, Cines DB, Higazi AA-R (2005) Plasminogen activators contribute to impairment of hypercapnic and hypotensive cerebrovasodilation after cerebral hypoxia/ischemia in the newborn pig. Stroke 36:2265–2269. https://doi.org/10.1161/01.STR.0000181078.74698.b0
50. Jagtap P, Szabó C (2005) Poly(ADP-ribose) polymerase and the therapeutic effects of its inhibitors. Nat Rev Drug Discov 4:421–440. https://doi.org/10.1038/nrd1718
51. Zhou T-B, Jiang Z-P (2014) Role of poly (ADP-ribose)-polymerase and its signaling pathway with renin-angiotensin aldosterone system in renal diseases. J Recept Signal Transduct Res 34:143–148. https://doi.org/10.3109/10799893.2013.865748
52. Satoh M, Date I, Nakajima M, Takahashi K, Iseda K, Tamiya T, Ohmoto T, Ninomiya Y et al (2001) Inhibition of poly(ADP-ribose) polymerase attenuates cerebral vasospasm after subarachnoid hemorrhage in rabbits. Stroke 32:225–231
53. English FA, McCarthy FP, Andersson IJ et al (2012) Administration of the PARP inhibitor Pj34 ameliorates the impaired vascular function associated with eNOS(−/−) mice. Reprod Sci 19:806–813. https://doi.org/10.1177/1933719111433885
54. Choi S-K, Galán M, Kassan M et al (2012) Poly(ADP-ribose) polymerase 1 inhibition improves coronary arteriole function in type 2 diabetes mellitus. Hypertension 59:1060–1068. https://doi.org/10.1161/HYPERTENSIONAHA.111.190140
55. Lenzsér G, Kis B, Snipes JA, Gáspár T, Sándor P, Komjáti K, Szabó C, Busija DW (2007) Contribution of poly(ADP-ribose) polymerase to postischemic blood-brain barrier damage in rats. J Cereb Blood Flow Metab 27:1318–1326. https://doi.org/10.1038/sj.jcbfm.9600437
56. Sekhon LH, Spence I, Morgan MK, Weber NC (1995) Chronic cerebral hypoperfusion in the rat: temporal delineation of effects and the in vitro ischemic threshold. Brain Res 704:107–111
57. Ishiguro M, Kawasaki K, Suzuki Y, Ishizuka F, Mishiro K, Egashira Y, Ikegaki I, Tsuruma K et al (2012) A Rho kinase (ROCK) inhibitor, fasudil, prevents matrix metalloproteinase-9-related hemorrhagic transformation in mice treated with tissue plasminogen activator. Neuroscience 220:302–312. https://doi.org/10.1016/j.neuroscience.2012.06.015
58. Mishiro K, Ishiguro M, Suzuki Y, Tsuruma K, Shimazawa M, Hara H (2012) A broad-spectrum matrix metalloproteinase inhibitor prevents hemorrhagic complications induced by tissue plasminogen activator in mice. Neuroscience 205:39–48. https://doi.org/10.1016/j.neuroscience.2011.12.042
59. Sehouli J, Braicu EI, Chekerov R (2016) PARP inhibitors for recurrent ovarian carcinoma: current treatment options and future perspectives. Geburtshilfe Frauenheilkd 76:164–169. https://doi.org/10.1055/s-0035-1558185
60. Dockery L, Gunderson C, Moore K (2017) Rucaparib: the past, present, and future of a newly approved PARP inhibitor for ovarian cancer. Onco Targets Ther 10:3029–3037. https://doi.org/10.2147/OTT.S114714